B. Erdmann [1]   C. Kober   J. Lang
P. Deuflhard   H.–F. Zeilhofer   R. Sader

Efficient and Reliable Finite Element Methods for Simulation of the Human Mandible

Efficient and Reliable Finite Element Methods for Simulation of the Human Mandible

Bodo Erdmann[1]   Cornelia Kober[2]   Jens Lang [3]
Peter Deuflhard[1]   Hans–Florian Zeilhofer[4]   Robert Sader[4]

Abstract

By computed tomography data (CT), the individual geometry of the mandible is quite well reproduced, also the separation of cortical and trabecular bone. Using anatomical knowledge about the architecture and the functional potential of the masticatory muscles, realistic situations can be approximated. The solution of the underlying partial differential equations describing linear elastic material behaviour is provided by an adaptive finite element method. Estimates of the discretization errors, local grid refinement, and multilevel techniques guarantee the reliability and efficiency of the method.

1   Introduction

A detailed understanding of the mechanical behaviour of the human mandible has been an object of medical and biomechanical research for a long time. Better knowledge of the stress and strain distribution, e.g. concerning standard biting situations, allows an advanced evaluation of the requirements for improved osteosynthesis or implant techniques. In the field of biomechanics, FEM-Simulation (FEM: finite element method) has become a well appreciated research tool for the prediction of regional stresses.

The scope of this paper is to demonstrate the impact of *adaptive finite element techniques* in the field of biomechanical simulation. Regarding to their

---

[1]Konrad-Zuse-Zentrum für Informationstechnik Berlin
[2]Center of Advanced Cranio-Maxillofacial Surgery, TU München
[3]Fachbereich Mathematik, TU Darmstadt
[4]Division of Cranio-Maxillofacial Surgery, University Hospital Basel

reliability, computationally efficient adaptive procedures are nowadays entering into real–life applications and starting to become a standard feature of modern simulation tools. Because of its complex geometry and the complicated muscular interplay of the masticatory system, modelling and simulation of the human mandible are challenging applications.

This research is part of a detailed simulation project concerning the human mandible. Descriptions of the simulation concept can be found in [11].

Previous FEM studies of the structural behaviour of human mandible have been reported for instance in Korioth et al. [13, 14] and Hart et al. [9]. Actually, there is a lot of advanced research concerning the interaction of the human mandible with dental implants, e.g. [19]. Since mainly commercial FEM tools are used in the field of biomechanics, adaptive finite elements are not wide spread here.

The paper is organized as follows. In Section 2, we explain the underlying simulation concept, including the mathematical model and the software. Then, in Section 3, we give a brief description of the theoretical background and the motivation of adaptive finite element techniques in this context. Afterwards, in Section 4, we describe and evaluate the results of our numerical experiments which consider a lateral bite based on previous biomechanical tests done by Moog [18]. Finally, in Section 5, we summarize the main features of our approach and give directions for future work.

2 The simulation concept

2.1 The model

In general, simulation in structural mechanics requires at least a representation of the specimen's geometry, an appropriate material description, and a definition of the load case. In our field, the inherent material is bone tissue, which is one of the strongest and stiffest tissues of the body. Bone itself is a highly complex composite material. Its mechanical properties are anisotropic, heterogeneous, and visco-elastic. At a macroscopic scale, two different kinds of bone can be distinguished in the mandible: cortical or compact bone is present in the outer part of bones, while trabecular, cancellous or spongious bone is situated at the inner, see Figure 1 [16, 19].

Computed tomography data (CT) are the base of the jawbone simulation. By this, the individual geometry is quite well reproduced, also the separation
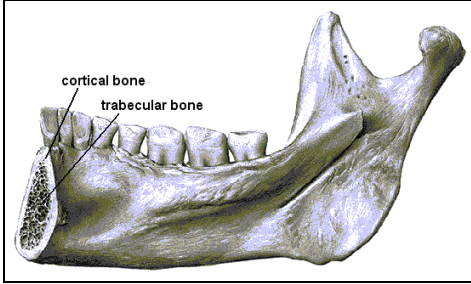
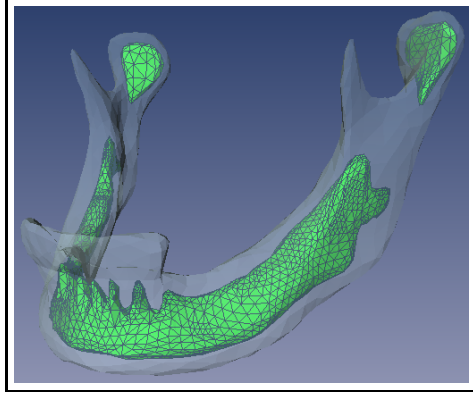Figure 1: The bone structure of the human mandible (from [20, 19]).

Figure 2: The separation of cortical and cancellous bone as realized in the simulations.

of cortical and trabecular bone, see Figure 2. The CT data give a density representation, but the three-dimensional information about the anisotropic material law is lost. In this note, we restrict ourselves to an isotropic, but inhomogeneous linear elastic material law. By this, at least in our setting, the choice of material parameter is of reduced impact. In the case of cortical bone, we refer to the experiments of [3]. A lot of experimentalists, for instance [27], postulate for the elastic moduli of trabecular bone about a tenth of the stiffness of cortical bone. Concerning the elastic coefficients of teeth, we use an average value of data available in standard literature.

We set

E = 13.3 GPa, ν = 0.224 for compact bone,

E = 1.33 GPa, ν = 0.224 for cancellous bone,

E = 16.0 GPa, ν = 0.224 for teeth.

Concerning anisotropic simulation, we refer to ongoing research activities of the group [10, 12].

The orientations and values of muscle and joint forces are taken from biomechanical experiments of Moog, see [18]. In Moog's setting, lateral biting consists of a combination of the musc. temporalis, the masseter-pterygoidus sling and condylar reaction forces, as given in Table 1. The FEM simulation requires as input a specification of force densities $[N/m^2]$ instead of force values $[N]$ as provided by Moog. Hence, we divide the given force data by appropriate muscle areas and set a constant force density for the muscles.

3

	Angle to the alveolar plane	Force value at the working side [N]	Force value at the balancing side [N]
Musc. temporalis	130	80	30
Masseter-pterygoidus sling	65	140	40
Temporo mandibular joint	-115	60	20

Table 1: muscular loading according to Moog's experiments [18].

Specific modifications are necessary to model the biting point, here the first premolar, see Figure 5. At genuine biting, some food (usually a highly non-linear material law) is crunched between the mandible and the maxilla. The chewing action itself is caused by muscles' activity and interactions going on in the temporo mandibular joint. Without any simplification, we would have to model a complex dynamic contact problem taking the lower part of the skull into account. The first simplification, also used by Moog, is a restriction to static situations. If we assume, as a worst case test, a very hard undeformable test specimen to be masticated, the upper and lower jaw rest immobile. By this, the restriction to a static situation, also used by Moog, is justified. In our setting, the teeth do only have the task of transferring the specimen's resistance to masticatory forces. Our purpose is the simulation of the jaw bone, not of the teeth. Therefore, we admit the test specimen to be a little cube perfectly adapted to the top of the tooth's shape. By this, we set approximately zero deformation at the biting point, leading to homogeneous Dirichlet boundary conditions there. Otherwise, a classical static signorini problem has to be considered, e.g. [22, 28, 15].

2.2 Algorithms and software

The main ingredients of the software concept are the visualization package $Amira^{TM}$ [25] for pre– and postprocessing including volumetric grid generation, and the adaptive FEM–code $Kaskade$ [1], both developed at the Zuse Institute Berlin.

Fully or even partially automated preprocessing of medical data is still a challenge. After semiautomatic segmentation of the CT data, the algorithm for generation of non-manifold surfaces provided by $Amira$ gives a quite satisfying reconstruction of the individual geometry, see Figure 4 (top left). Volumetric mesh generation based on these surface grids would exceed the ca-

pacities of commonly available simulation tools and still allows obtuse angles which are disadvantageous in the finite element approximation. Therefore, the next steps are successive grid coarsening, smoothing, and interactive grid editing in order to improve mesh quality. A simplification algorithm from computer graphics [8] has been adapted for this purpose, specially avoiding intersections and assuring a high quality (i.e. small aspect ratio) of the surface triangles. Finally, volumetric tetrahedral meshes suitable for FEM-simulation can be generated using an advancing front algorithm. For the theoretical background, we refer to [24, 26, 21].

As mentioned above, the FEM–simulation itself is done by means of *Kaskade* ([6], [4]). This adaptive finite element code provides automatic grid refinement during the calculation in order to compute solutions with high accuracy. After successfull FEM–calculation, the results are again transferred to *Amira* for visualization, see also Section 4.2.

3   Adaptive finite element methods

In the study of human mandible, the governing physical laws are the three–dimensional equations of linear elasticity. We are using linear finite element methods with tetrahedral meshes for the numerical solution of these stationary partial differential equations. Tetrahedral meshes allow us to get a faithful representation of the complicated tissue boundaries. Linear finite elements are suffiently accurate due to the roughness of the deformation caused by mixed boundary conditions.

Typically, for a given application, we seek to obtain a desired result via an efficient reliable simulation. Therefore, our finite element algorithms are based on adaptive mesh refinement [6], i.e. the finite element grid is automatically improved in regions where the numerical solution does not have the required accuracy. Adaptive techniques are driven by error estimators, which yield an estimate of the local discretization error in the calculated displacements. Efficient implementation of adaptive mesh refinement requires particular attention to the supporting data structures and algorithm complexity [7].

Adaptive techniques are playing an increasingly important role in the area of computational science. Numerical and modelling errors can be clearly distinguished with the effect that reliability of the modelling process can be assessed. Compared to uniform methods, successful adaptive methods lead to substantial savings in computational work for a given error tolerance. We consider these procedures of crucial importance, as the user is released from

constructing problem–specific discretizations and checking the reliability of the numerical solution.

4 Results

The simulation examples in this section are based on the generally available CT data set of the female visible human project, see [2].

4.1 Successive grid coarsening and refinement

The surface representation provided by the algorithm of *Amira*, see Figure 4 (top left), consists of 48,558 points, resp. 97,247 faces. The result of some coarsening steps is shown in Figure 4 (bottom left). The corresponding tetrahedral grid has 11,395 tetrahedra resp. 2,632 points and is used as a starting (level 0) grid in the adaptive calculation. According to the requirements of the selected load case, here the lateral biting situation, the volumetric grid is successively refined from level 0 up to level 4, see Figure 4.

level	Points	x–Deformation	y–Deformation	z–Deformation
0	2632	-9.70e-5 − 3.81e-4	-1.49e-4 − 1.99e-4	-1.37e-5 − 6.43e-4
1	5767	-1.71e-4 − 5.05e-4	-2.90e-4 − 2.87e-4	-1.85e-5 − 1.06e-3
2	13714	-2.33e-4 − 6.14e-4	-4.20e-4 − 3.68e-4	-2.17e-5 − 1.40e-3
3	32236	-2.63e-4 − 6.63e-4	-4.82e-4 − 4.08e-4	-2.22e-5 − 1.56e-3
4	78394	-2.75e-4 − 6.81e-4	-5.22e-4 − 4.31e-4	-2.37e-5 − 1.64e-3

Table 2: Range of deformation during adaptive refinement.

level	Points	x–Deformation	y–Deformation	z–Deformation
0	2632	-9.70e-5 − 3.81e-4	-1.49e-4 − 1.99e-4	-1.37e-5 − 6.43e-4
1	17974	-1.75e-4 − 5.40e-4	-2.85e-4 − 2.94e-4	-1.90e-5 − 1.08e-3
2	132371	-2.38e-4 − 6.45e-4	-4.32e-4 − 3.77e-4	-2.21e-5 − 1.43e-3

Table 3: Range of deformation during uniform refinement.

A more detailed convergence history is listed in Table 2. The corresponding results for some steps based on uniform refinement are shown in Table 3. In Figure 3, we present the maximum absolute values of deformation (occuring in the processus coronoidus) for both adaptive and uniform refinement of the grid. The comparison makes it comprehensible that the adaptive method is much more efficient if high accuracy is required.
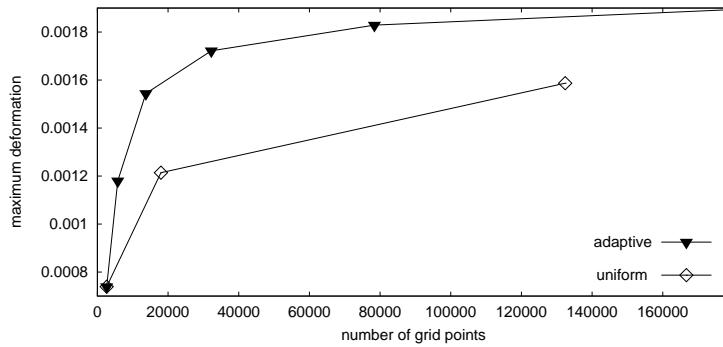
Figure 3: Adaptive versus uniform mesh refinement: comparative maximum deformation results.

Figure 5 gives a combined presentation of the deformed mandible (100–times exaggerated) and the original undeformed geometry.

4.2 Appropriate postprocessing

Kaskade computes the three–dimensional deformation and also the six components of the stress and the strain tensor. In general, the choice of the postprocessing variables to be plotted and examined is highly decisive. In the following, the results after adaptive calculation of some common post processing variables are discussed. Because of the only auxiliary meaning of the teeth in our simulation, they are omitted in the visualization.

The von Mises equivalent stress represents the distortional part of the strain energy density for isotropic materials. It has been used to predict the yield of isotropic, ductile materials with good empirical agreement. Numerous experiments, e.g. [5], show that cortical and also trabecular bone exhibit creep behaviour somehow associated to metals or ceramics. So, the calculation of the von Mises equivalent stress is of a certain – but because of its restriction on isotropic media limited – impact. Figure 6 and 7 show a comparison between the results of a calculation of level 0 versus level 4. In both calculations, the stress maximum occurs around the processus coronoidus of the working side whereas the condyles are nearly at the minimum level in spite of the condylar reaction forces according to Moog's experiments [18]. In the level 0 calculation, the observed stress maximum of 2.81 MPa is about 65 % less than the maximal stress of 4.34 MPa achieved in the level 4 calculation.

Experiments and simulations done in [23] suggest that measurements of bone
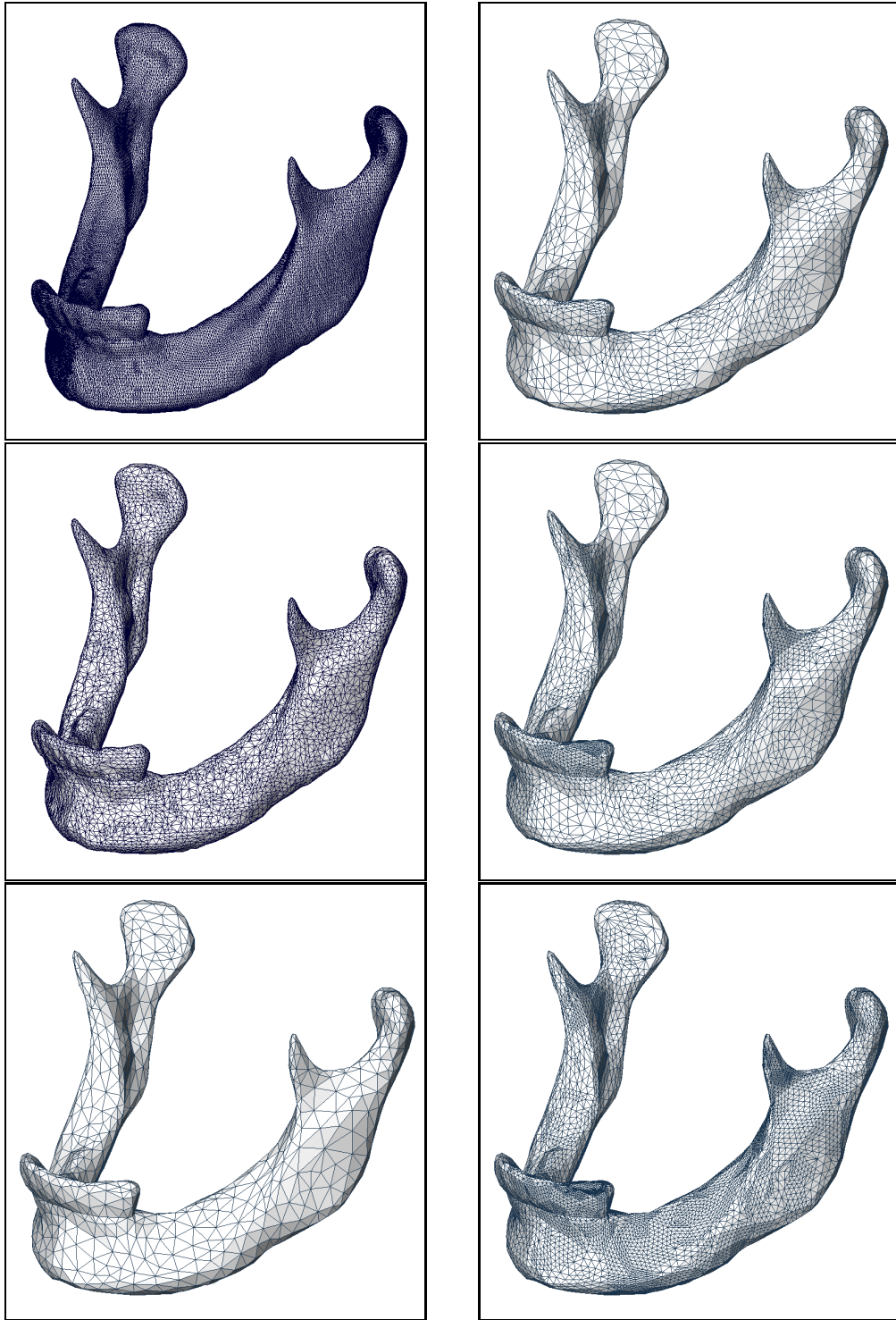
Figure 4: Left column: 3 levels of coarsening of grid by *Amira*, left
bottom: initial (level 0) grid, right column: level 1, 2, and 3 in the
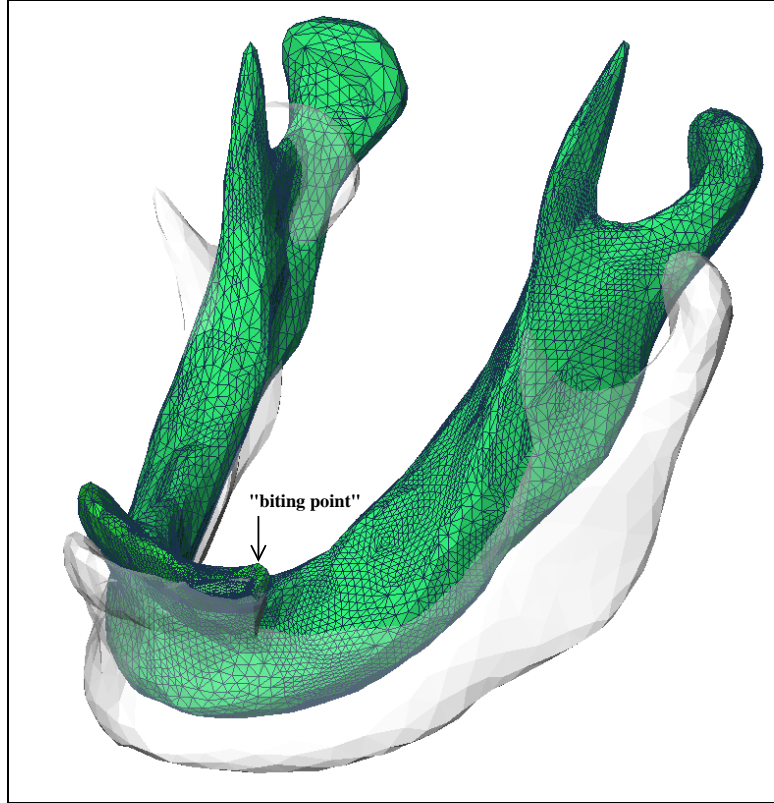adaptive refinement process by *Kaskade*.

Figure 5: Level 3 of adaptive refinement, together with a 100–times exaggerated visualization of the deformed geometry in the course of lateral biting. The original geometry is shown transparently.

strain are more relevant to predict local fracture than those of bone stress. Therefore, we additionally test the impact of adaptive grid refinement on volumetric strain, see Figure 8 and 9. The comparison of the level 0 and level 4 results confirms the previous observation concerning the von Mises equivalent stress. Both calculations show qualitatively similar results, but a significant quantitative deviance which is dimished in the case of compressive strain, e.g. near the biting point and also in the incisura mandibulae. Specially, for anisotropic media, Hart et al. propose in [9] a mechanical intensity scalar, defined as the product of the sign of volumetric strain and square root of the strain energy density. These postprocessing variables are visualized in Figure 10 and 11.
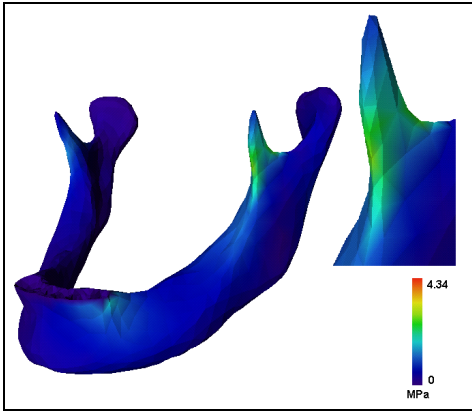
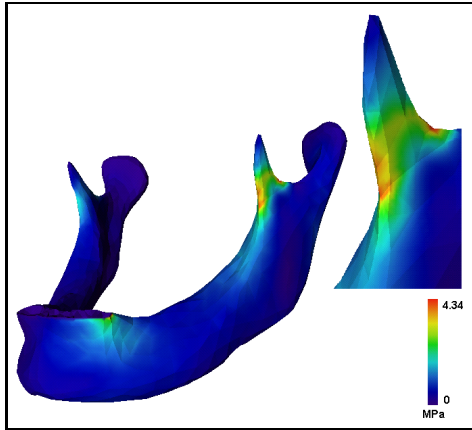Figure 6: Von Mises equivalent stress, after level 0–calculation, maximum: 2.81e+06.

Figure 7: Von Mises equivalent stress, after level 4–calculation, maximum: 4.34e+06.
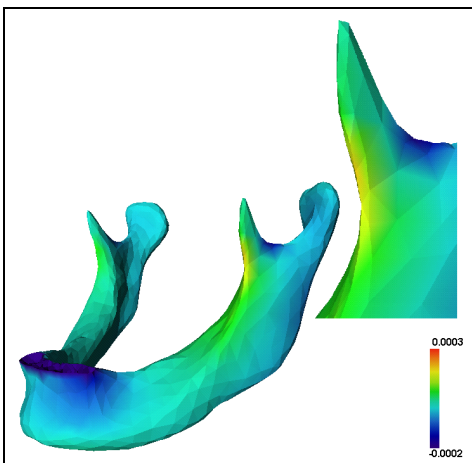

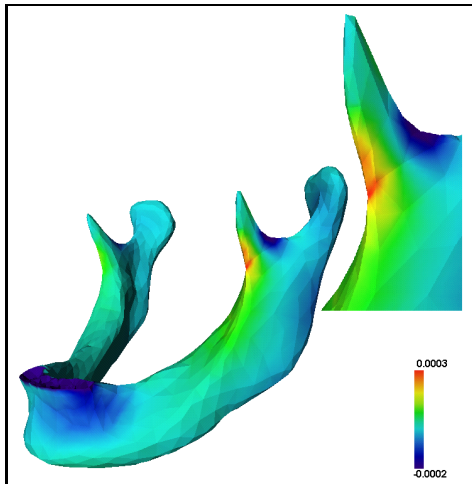Figure 8: Volumetric strain, after level 0–calculation.

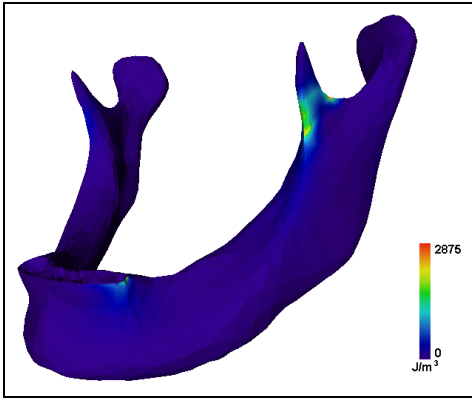Figure 9: Volumetric strain, after level 4–calculation.

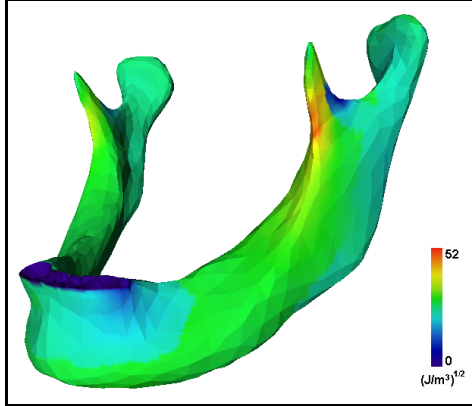Figure 10: Strain energy density, after level 4–calculation.

Figure 11: Mechanical intensity, after level 4–calculation.

5   Conclusion and outlook

The purpose of this paper is to demonstrate the impact of adaptive finite element techniques in biomechanical simulation. A lateral biting situation serves as an application example. By successive grid refinement, the deformation shows good convergence from the third level of refinement.

Concerning some widely used postprocessing variables, like von Mises equivalent stress, volumetric strain or elastic energy density, we observed qualitatively similar results of the level 0 and the level 4 calculations, but quantitatively large deviances which justify the use of more sophisticated numerical concepts as presented here.

After careful evaluation, the authors will combine adaptive finite element methods with anisotropic material simulation based on ongoing research studies of the group [12]. Furthermore, the simplified test setting of the masticatory system will be replaced by more realistic models, e.g. [17].

6   Acknowledgement

References

[1] `http://www.zib.de/SciSoft/kaskade`

[2] National Library of Medicine. The Visible Human Project, `http://www.nlm.nih.gov/research/visible/visible_human.html`, 1995.

[3] R.B. Ashman, W.C. Van Buskirk: The elastic properties of a human mandible. Adv. Dent. Res. 1 (1987), pp. 64-67.

[4] F. Bornemann, B. Erdmann, R. Kornhuber: Adaptive multilevel-methods in three space dimensions, Int. J. Num. Meth.in Eng, Vol. 36, (1993), pp. 3187-3203.

[5] S. Bowman, T. Keaveny, L. Gibson, W. Hayes, T. McMahon: Compressive creep behaviour of bovine trabecular bone. J. Biomech., 27 (1994), pp. 301-310.

[6] P. Deuflhard, P. Leinen, H. Yserentant: Concepts of an Adaptive Hierarchical Finite Element Code. IMPACT Comp. Sci. Eng. 1 (1989), pp. 3-35.

[7] B. Erdmann, J. Lang, R. Roitzsch: KASKADE–Manual, Technical Report TR 93-05, Konrad–Zuse–Zentrum Berlin (ZIB), 1993.

[8] M. Garland, P.S. Heckbert: Surface Simplification using quadratic error metrics, in Computer Graphics (Proc. SIGRAPH '97), pp. 209-216.

[9] R.T. Hart, V.V. Hennebel, N. Thongpreda, W.C. van Buskirk, R.C. Anderson: Modeling the Biomechanics of the Mandible: A Three-Dimensional Finite Element Study. J. Biomechanics, 25 (1992), pp. 261-286.

[10] C. Kober, R. Sader, H. Thiele, H.-J. Bauer, H.-F. Zeilhofer, K.-H. Hoffmann, H.-H. Horch: The influence of anisotropic microstructure of bone on macroscopic FEM-simulation of the human mandible. ACAS 99, Augustusburg 1999.

[11] C. Kober, R. Sader, H. Thiele, H.-J. Bauer, H.-F. Zeilhofer, K.-H. Hoffmann, H.-H. Horch: A modular software concept for the individual numerical simulation (FEM) of the human mandible. Biomed. Technik 45 (2000), pp. 119-125.

[12] C. Kober, R. Sader, H.-F. Zeilhofer, S. Prohaska, S. Zachow, P. Deu-flhard: Anisotrope Materialmodellierung im menschlichen Unterkiefer, 8. Workshop "Die Methode der Finiten Elemente in der Biomedizin, Biomechanik und angrenzenden Gebieten" der Universität Ulm, 2001.

[13] T.W. Korioth, D. P. Romilly, A. G. Hannam: Three Dimensional Finite Element Stress Analysis of the Dentate Human Mandible. Am. J. of Physical Anthropology 88 (1992), pp. 69-96.

[14] T.W. Korioth, A. Versluis: Modeling the mechanical behaviour of the jaws and their related structures by finite element (FE) analysis. Crit. Rev. Oral Biol. Med. 8 (1997), pp. 90-104.

[15] R. Kornhuber, R. Krause: Adaptive Multigrid Methods for Signorini's Problem in Linear Elasticity, Preprint Nr. A-15-2000 (2000), FU Berlin, to appear in: Comp. Vis. Sci..

[16] R.B. Martin, D.B. Burr, N.A. Sharkey: Skeletal Tissue Mechanics, Springer–Verlag, New York Berlin Heidelberg, 1998.

[17] Ch. Meyer: Photoelastomechanische Analyse des Kiefergelenks, "Medicine Meets Mathematics, Hartgewebe-Modellierung", Kloster-Banz/Staffelstein, 2001.

[18] T. Moog: Spannungsoptische Untersuchungen an unverletzten und frak-turierten Unterkiefern, Ph. D. Thesis, Univ. Würzburg, 1991.

[19] H. van Oosterwyck: Study of biomechanical determinants of bone adap-tion around functionally loaded oral implants, Ph.D. thesis, Katholieke Universiteit Leuven, Faculteit Toegepaste Wetenschappen, Department Werktuigkunde Afdeling Biomechanica en Grafisch Ontwerpen, 2000.

[20] R. Putz, R. Pabst: Sobotta atlas of human anatomy, Urban & Schwarzenberg, Munich, Vienna, Baltimore, 1994.

[21] M. Seebaß, R. Beck, J. Gellermann, J. Nadobny, P. Wust: Electro-magnetic phased arrays for regional hyperthermia – optimal frequency and antenna arrangement, Report 00-28, Konrad–Zuse–Zentrum Berlin (ZIB), 2000.

[22] A. Signorini: Sopra alcune questioni di elastistatica. Atti della Societa Italiana per il Progresso della Scienze, 1933.

[23] M.J. Silva, T.M. Keaveny, W.C. Hayes: CT-based finite element analysis predicts failure loads and fracture patterns for vertebral sections. Trans. Orthop. Res. Soc., 273 (1996), pp. 234-242.

[24] D. Stalling, M. Seebass, S. Zachow: Mehrschichtige Oberflächenmodelle zur computergestützten Planung in der Chirugie. Technical Report TR 98-05, Konrad–Zuse–Zentrum Berlin (ZIB), 1998.

[25] D. Stalling, M. Zöckler, H.-C. Hege: AMIRA – Advanced Visualization, Data Analysis and Geometry Reconstruction. `http://amira.zib.de`.

[26] D. Stalling, M. Zöckler, H.-C. Hege: Segmentation of 3D Medical Images with Subvoxel Accuracy, in: H.U. Lemke, K. Inamura, M.W. Vannier, A.G. Farman (eds), Proc. CAR'98 Computer Assisted Radiology and Surgery, Tokyo, 1998, pp. 137-142.

[27] G.E.O. Widera, J.A. Tesk, E. Priviter: Interaction effects among cortical bone, cancellous bone and peridontal membrane of natural teeth and implants, J. Biomed. Mater. Res. Symp. 7 (1976), pp. 613-623.

[28] P. Wriggers: Finite element algorithms for contact problems. Arch. Comp. Meth. Engrg., 2 (1995), pp.1-49.